Supporting Information

Solar Energy Harvesting in Type II van der Waals Heterostructures of Semiconducting Group III Monochalcogenide Monolayers

Ashima Rawat, Raihan Ahammed, Dimple, Nityasagar Jena, Manish Kumar Mohanta and Abir De Sarkar*

Institute of Nano Science and Technology, Phase 10, Sector 64, Mohali, Punjab-160062, India

*E-mail: abir@inst.ac.in; abirdesarkar@gmail.com

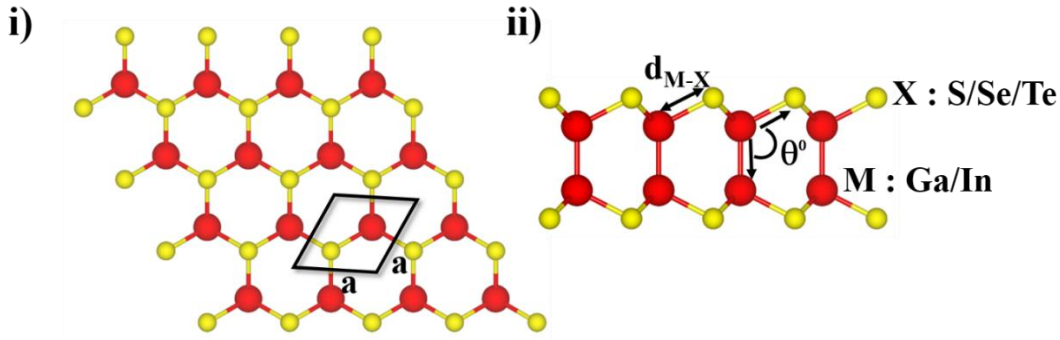

Figure S1. Lattice structure of Group IIIA-VIA monolayer (MX; M=Ga, In; X=S, Se, and Te): (i) top view of the monolayer with hexagonal supercell with the zig-zag direction along x axis and the armchair direction along the y axis (ii) side view of the monolayer lattice structure where d_{M-X} represents the bond length and θ is the bond angle in degrees.

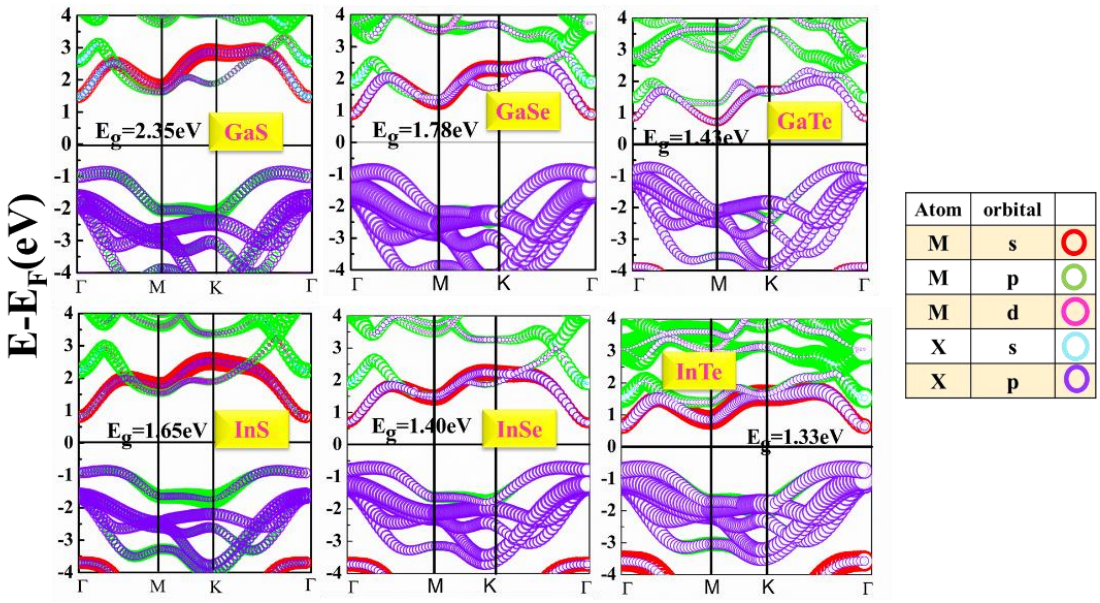

Figure S2. Partial Bandstructure projection of Group III monolayers using PBE functional where M: Ga/In and X: S/Se/Te. The colored symbols show the band from the different orbitals. The size of each symbol is proportional to the weight of the band eigenfunctions on different orbitals.

Table S1 Work function for the Group III monolayers in eV

ML	**GaS**	**GaSe**	**GaTe**	**InS**	**InSe**	**InTe**
E.A.	5.36	4.90	4.58	5.53	5.24	4.74

Optical Property:

The absorption coefficient of a particular monolayer can be obtained using the formula $\alpha_{abs} = \frac{\sqrt{2}\omega}{c}\left(\left(\sqrt{\varepsilon_1^2(\omega)+\varepsilon_2^2(\omega)}-\varepsilon_1(\omega)\right)\right)^{1/2}$,where $\varepsilon_1(\omega)$ and $\varepsilon_2(\omega)$ are the real and imaginary parts of the frequency dependent dielectric function, $\varepsilon(\omega)$ respectively.The Figure S2 shows the absorption spectra for all the six monolayers.

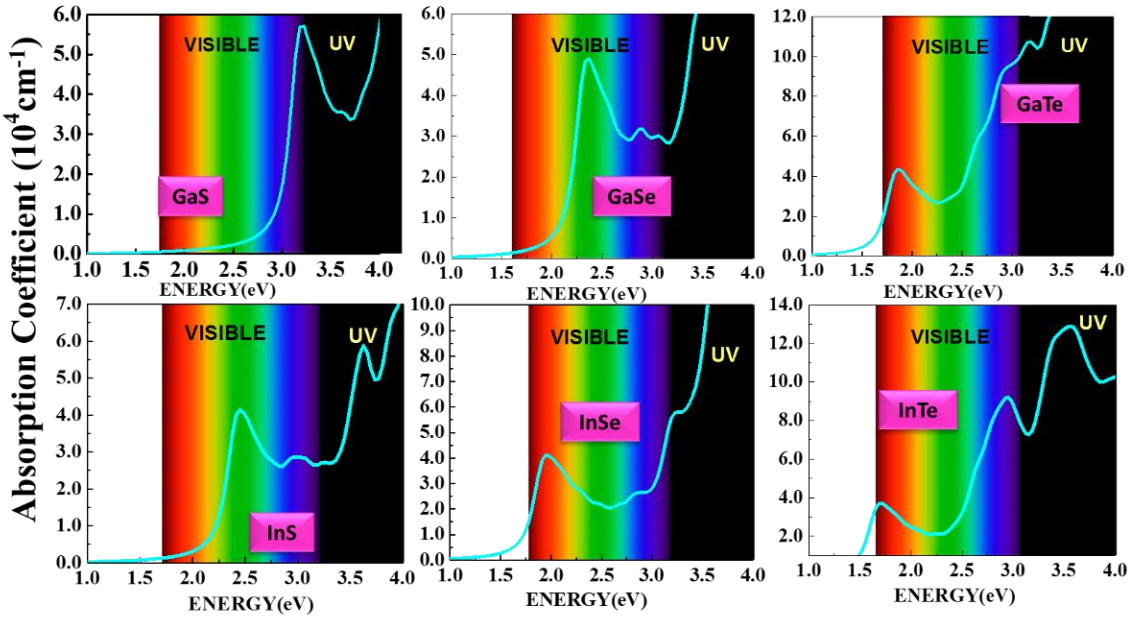

Figure S3. Absorption coefficient for the monolayers in the visible and UV region of the solar spectrum.

Table S2. Binding energy, E_b for various stacking modes in various Heterostructures.

E_b (meV/Å^2)	STACKING A	STACKING B	STACKING C
GaTe/InTe	-18.05	-14.15	-13.47
GaTe/InS	-11.38	-20.49	-16.92
GaSe/InS	-17.89	-24.80	-06.68
GaTe/InSe	-15.20	-13.12	-07.59

InS/InSe

Photocatalysis

From the Figure S4 a) we can note that the water splitting character of the heterostructure is feasible around a pH value of 0-2 thereby making it highly sensitive to the catalytic environment. The absorption spectra in Figure S4b shows an excitonic peak around 2.5 eV and the main absorption peak around 3.1 eV which lies towards the edge of the visible region. Hence, it will also absorb optimum solar energy to act as a good photocatalyst.

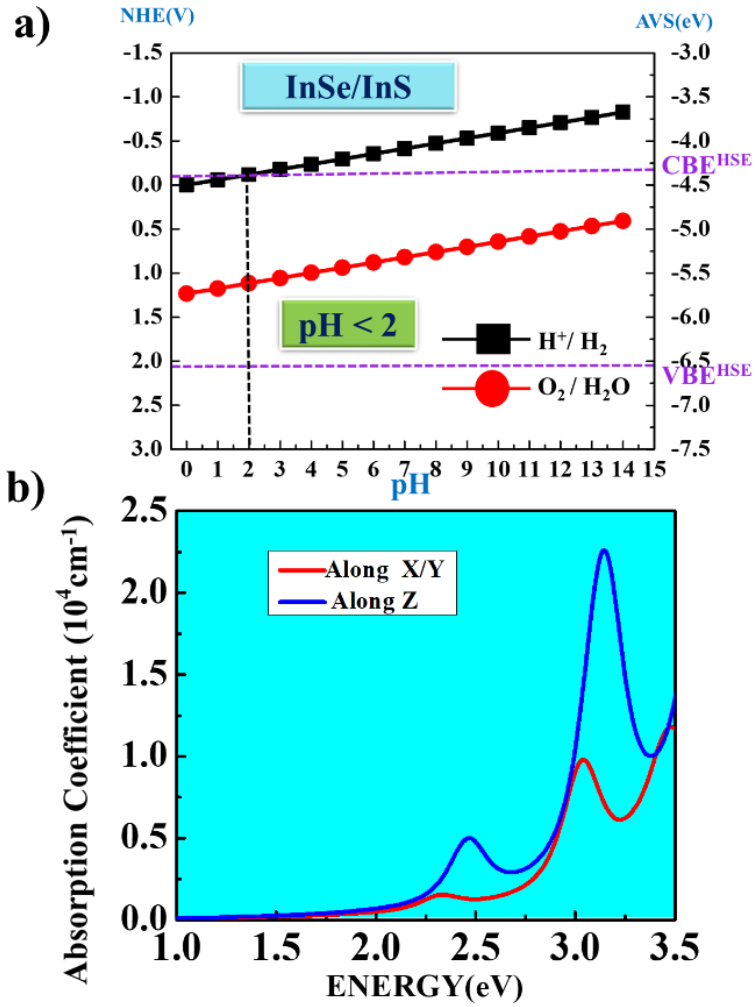

Figure S4. a) Effect of pH on the redox potentials for H_2O splitting in the absolute vacuum scale (AVS) and normal hydrogen electrode (NHE) potential [The band edges have been shown via dotted lines. CBE and VBE denote conduction and valence band edge respectively.], b) Absorption coefficient of the heterostructure in the in plane and out of plane directions.

GaTe/InS

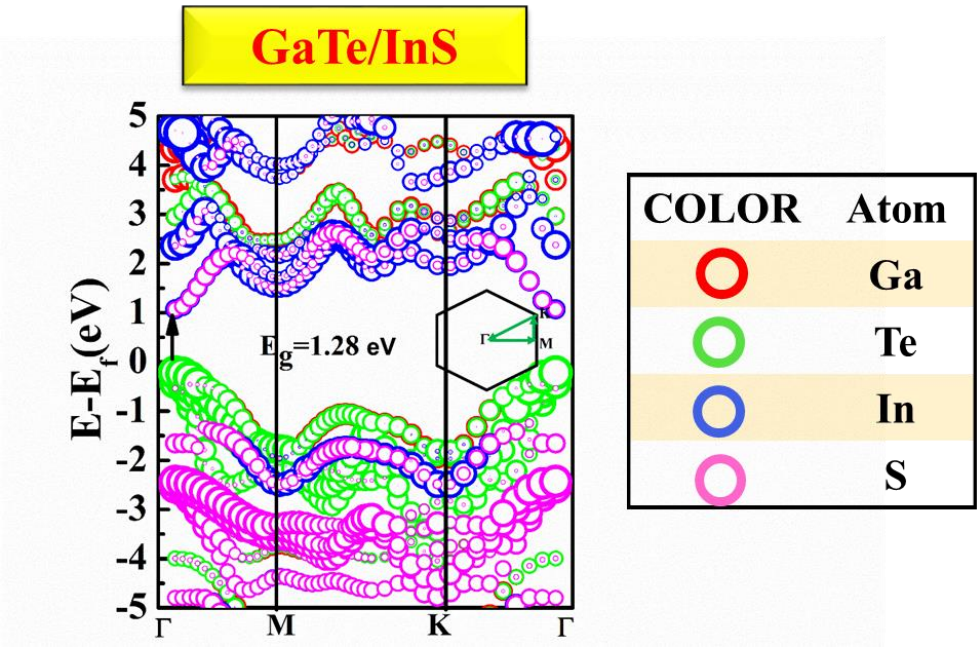

Figure S5. Bandstructure of GaTe/InS heterostructure calculated using HSE06 functional where the size of each symbol is proportional to the weight of the band eigenfunctions on different orbitals.

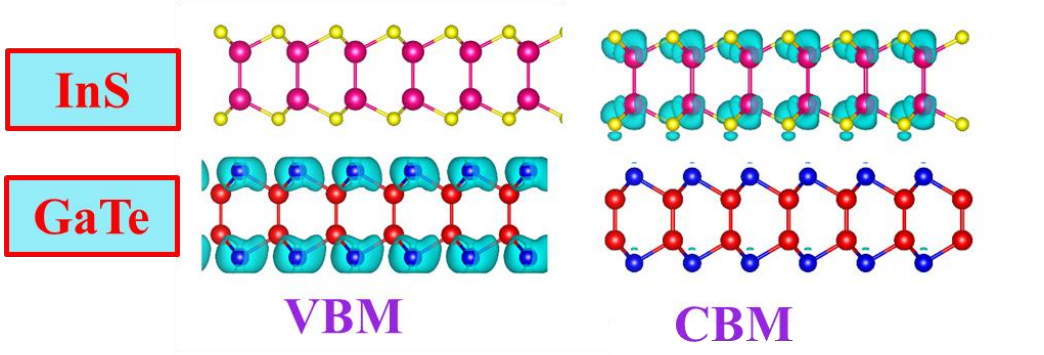

Figure S6. Band decomposed charge density plot at the band edges CBM (conduction band minima) and VBM (valence band maxima) at an isosurface value of 0.5 X 10^{-4} e/Å^3

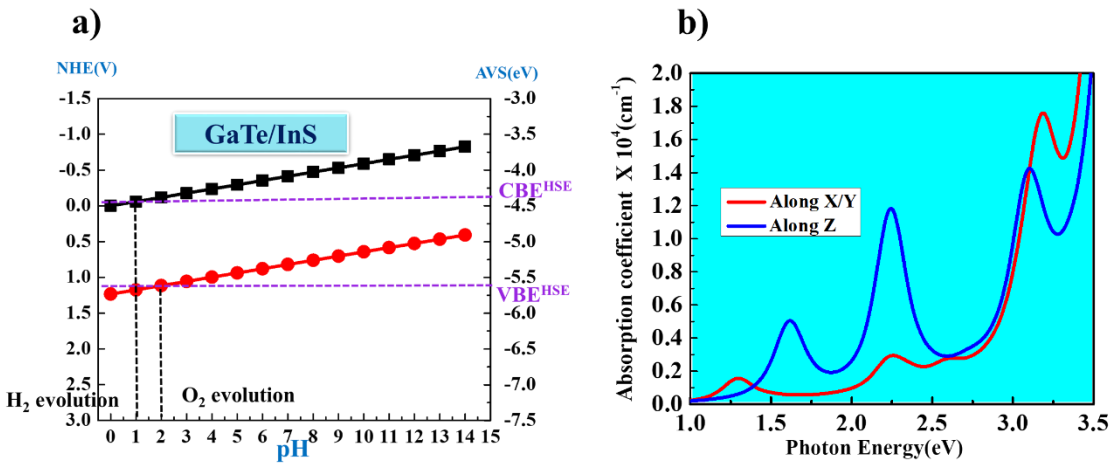

Figure S7. a) Effect of pH on the redox potentials for H_2O splitting in the absolute vacuum scale (AVS) and normal hydrogen electrode (NHE) potential (The band edges have been shown via dotted lines. CBE and VBE denote conduction and valence band edge respectively), b) Absorption coefficient of the heterostructure in the in plane and out of plane directions.

The band structure of GaTe/InS heterostructure is again calculated using the HSE06 functional with shows a direct bandgap of 1.28eV at the Gamma point as shown in Figure S5. It is interesting to note that there is a transition from indirect to direct bandgap as the monolayers are having indirect bandgap in their pristine form while the hetero-bilayer is a direct bandgap. From Figure S5 we can also observe that the valence band edge depends on the Te atom of GaTe monolayer and conduction band edge on the S atom of the InS monolayer confirming the staggered type nature of the heterostructure. The band-decomposed charge density shows the contribution to the bandedges from the different monolayers. Hence, the electrons are centred on the GaTe monolayer whereas the holes are centred on the InS which is evident from Figure S6. The main drawback of this of this particular heterostructure is the range of pH for H_2 and O_2 evolution is different. As can be seen from the Figure S7a the H_2 evolution can take place in the acidic medium (pH< 2) and O_2 evolution in the acidic to basic medium. The absorption spectra also shows the main peak around 2.2 eV, which indicates a good amount of visible light absorption. Hence, this particular heterostructure can be utilised for H_2/O_2 production efficiently.

GaTe/InSe

The bandstructure of GaTe/InSe heterostructure is described in Figure S8.

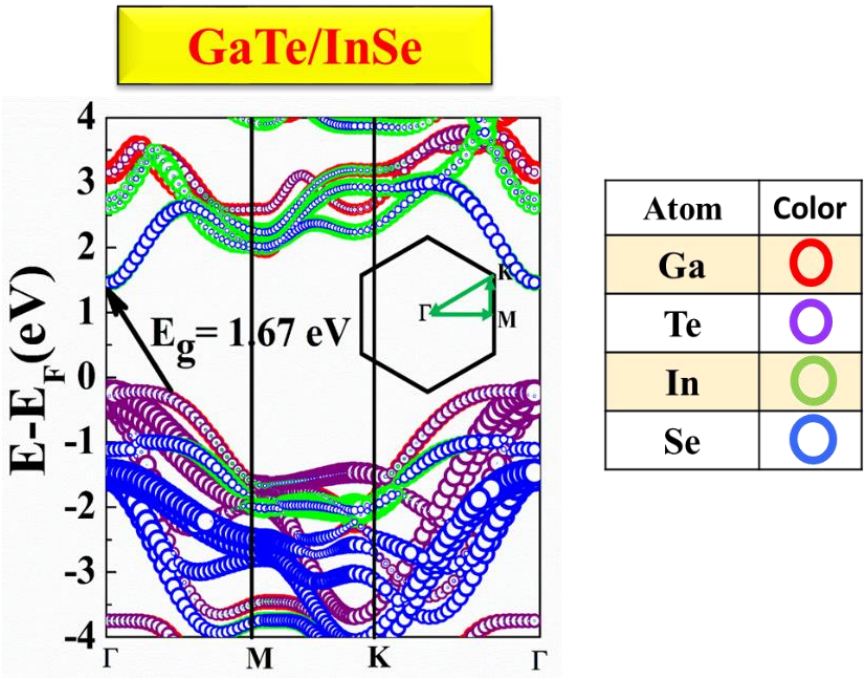

Figure S8. Bandstructure of GaTe/InSe heterostructure calculated using HSE06 functional the size of each symbol is proportional to the weight of the band eigenfunctions on different orbitals.

In the bandstructure for the heterostructure it can be observed that the valence band maxima depends on the Te atom of GaTe monolayer and the conduction band minima on the Se atom of the InSe monolayer confirming the staggered type nature of the heterostructure. The indirect bandgap of the heterostructure is found to be 1.67 eV. The band-decomposed charge density of states in Figure S9 clearly shows the charge contribution to the band edges from the different monolayers. The electron charge is centred around the InSe monolayer whereas the hole charge distribution is centred around the GaTe monolayer.

The binding energy is found to the -15.20 meV/$Å^2$at a vdW gap of 3.94 Å thereby making it highly stable under normal conditions.

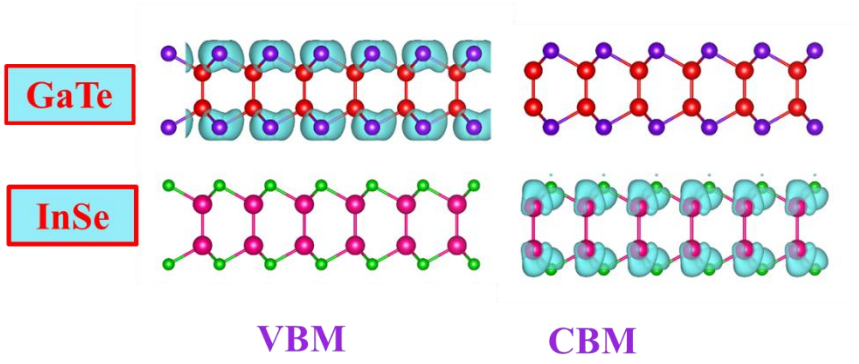

Figure S9. Band decomposed charge density plot at the band edges CBM (conduction band minima) and VBM (valence band maxima) at an isosurface value of 1.4 X 10^{-4} e/Å^3

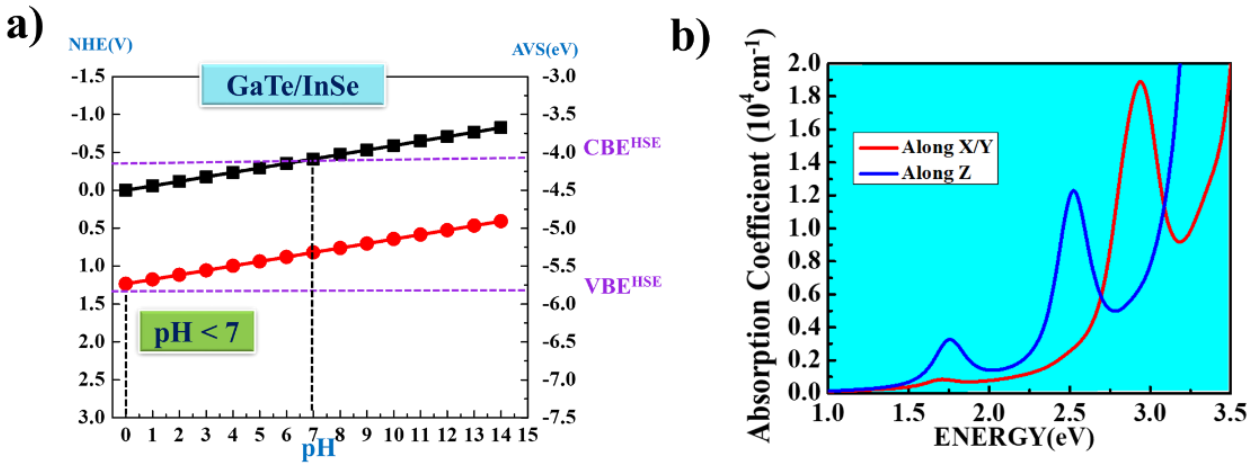

Figure S10. a) Effect of pH on the redox potentials for H_2O splitting in the absolute vacuum scale (AVS) and normal hydrogen electrode (NHE) potential [The band edges have been shown via dotted lines. CBE and VBE denote conduction and valence band edge respectively.], b) Absorption coefficient of the heterostructure in the in-plane and out-of-plane directions**.**

Further, we have studied its application in photocatalytic water splitting. The important factor for the photocatalysis is the straggling of the redox potential by the band edges. The Figure S10a predicts the H_2 and O_2 evolution in GaTe/InSe as a potential photocatalyst with variation in pH. The heterostructure is capable of splitting the water around a pH value of 0-7. In addition to this the absorption coefficient of the heterostructure has been considered to observe their capacity to absorb solar spectrum. From Figure S10b we can observe that the excitonic peak in the plot around 1.6 eV and main absorption peaks arises around 2.4 eV which suggests the optimum absorption of

the visible photons for photocatalysis. Also, there is a substantial absorbance in the out of plane (z axis) as well in addition to the in plane solar absorption.

GaSe/InS

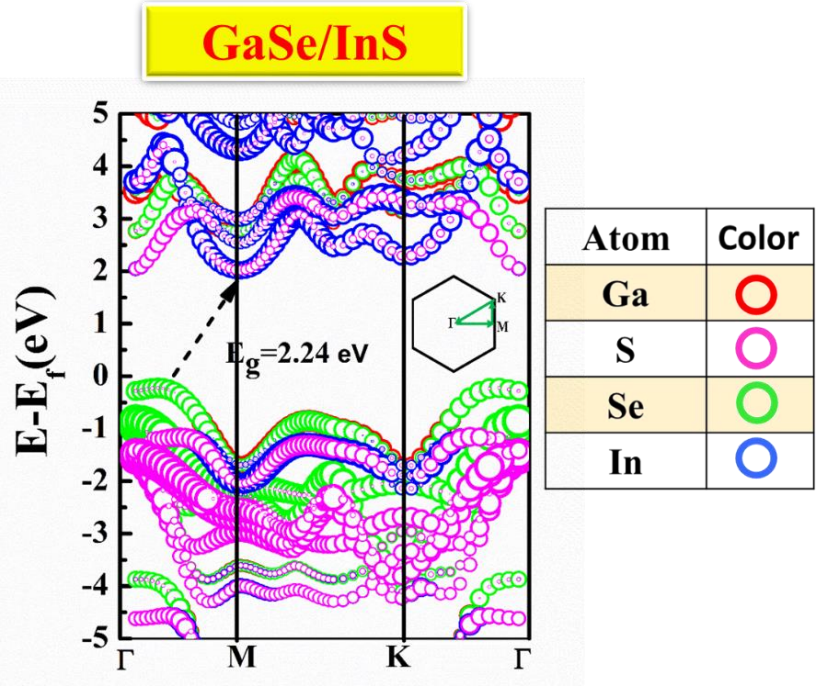

Figure S11. Band structure of GaSe/InS heterostructure where the size of each symbol is proportional to the weight of the band eigenfunctions on different orbitals**.**

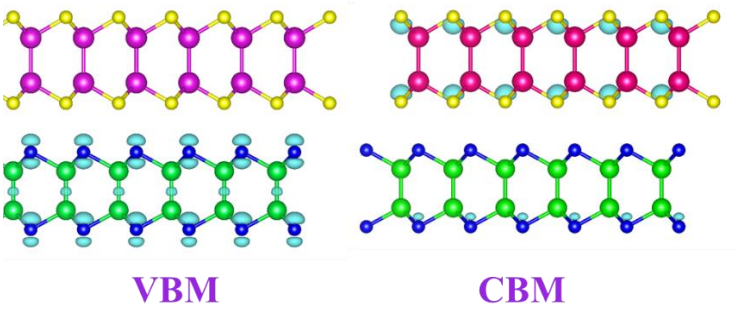

Figure S12. Band decomposed charge density plot at the band edges CBM (conduction band minima) and VBM (valence band maxima) at an isosurface value of 0.3 X 10^{-3} e/Å^3 **.**

From the band decomposed charge distribution at the band edges in figure S12 it can be verified that it is a staggered type heterostructure since the majority charges are centered on the different

monolayers at the band edges of the heterostructures. The van der Waals gap between the monolayers of the heterostructure i.e. 3.12 Å and the binding energy is found to be around -24.80 meV/Å^2.

Phonon Calculations:

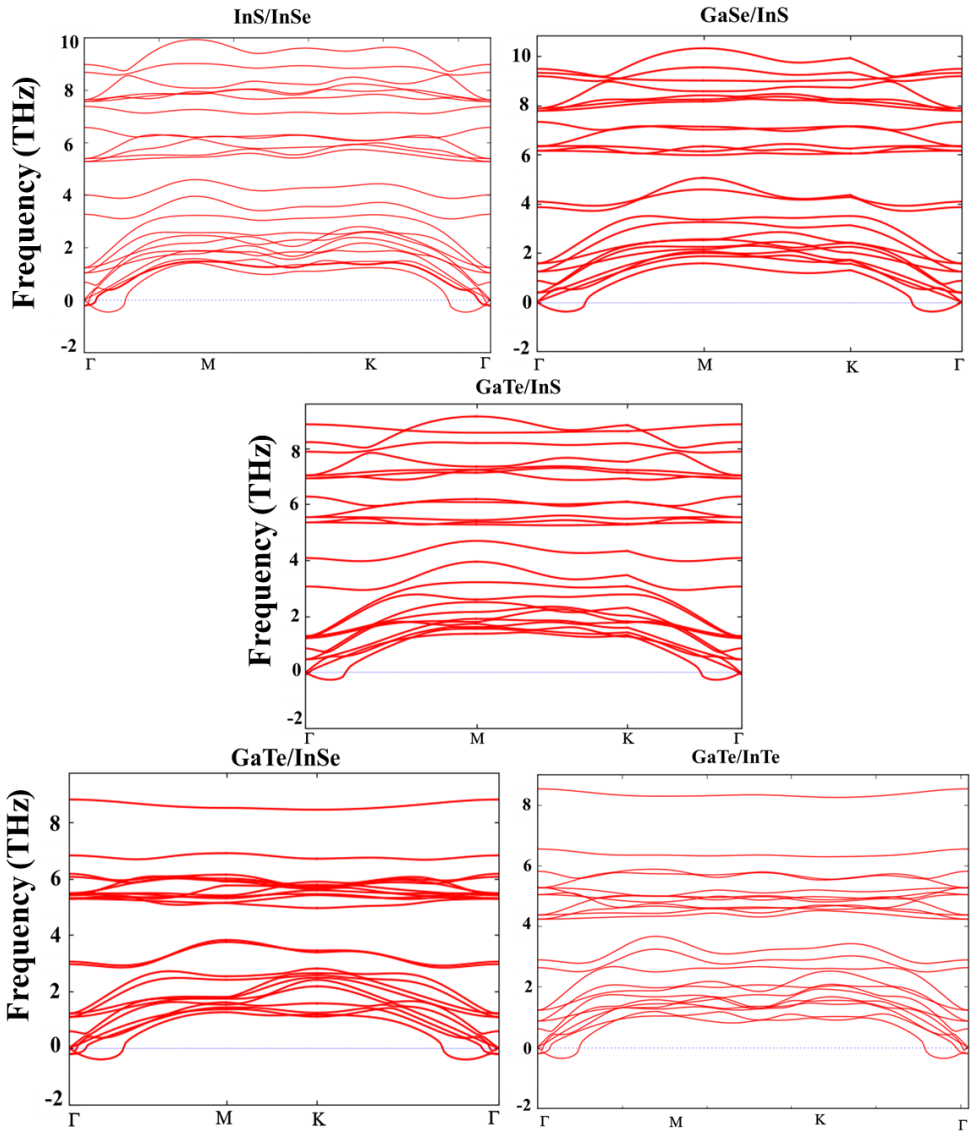

Figure S13. Phonon band dispersion in the hetero-bilayers calculated using PHONOPY.

PCE using the Macroscopic Average Potential (GaTe/InSe)

Table S3. The values of VBM (CBM) valence band edges (conduction band edge), vacuum, VBM_vac (CBM_vac) valence band edge (conduction band edge) with respect of vacuum,$\bar{\bar{V}}$

macroscopic potential, VBM_$\bar{\bar{V}}$(CBM_$\bar{\bar{V}}$) valence band edge (conduction band edge) with respect of macroscopic potential. E_g bandgap of the monolayers under strained environment in the heterostructure in eV.

HS	VBM	CBM	Vacuum	VBM_vac	CBM_vac	$\bar{\bar{V}}$	VBM_$\bar{\bar{V}}$	CBM_$\bar{\bar{V}}$	E_g
GaTe	2.16	-0.21	1.55	0.61	-1.76	13.58	-12.97	-15.34	2.37
InSe	2.16	-0.23	1.52	0.64	-1.75	13.46	-12.82	-15.20	2.39

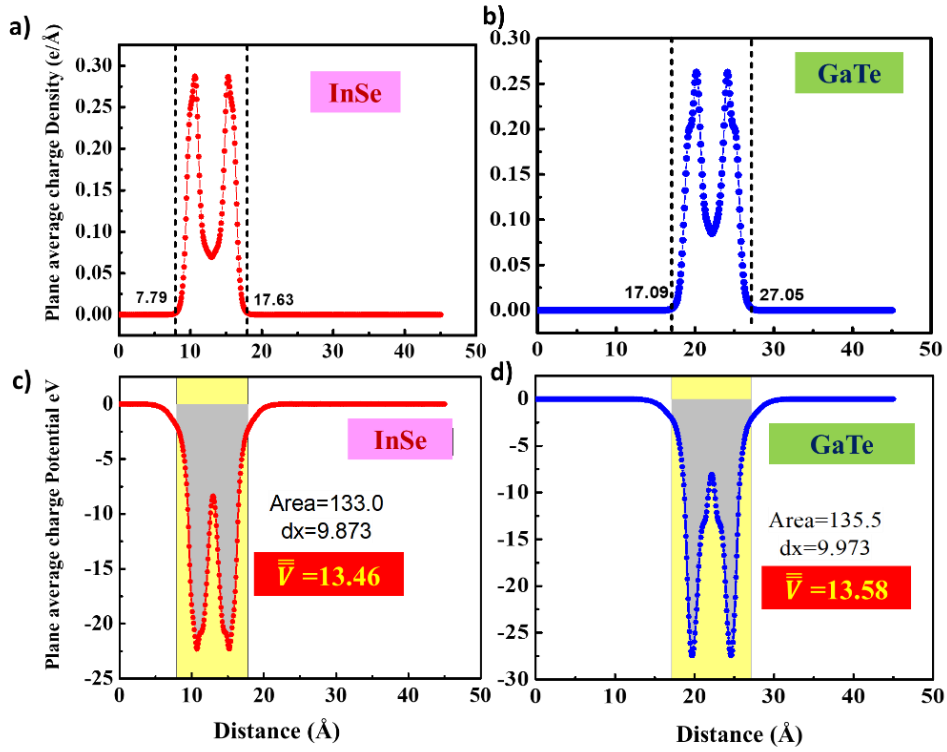

Figure S14. Plane average charge density (a and b) and electrostatic potential, $\bar{V}$ (c and d) of the InSe and GaTe monolayers along the z direction in strained heterobilayers (arising from x% lattice mismatch between the individual monolayers). $\bar{\bar{V}}$ in the inset in c) and d) represent the macroscopic plane average potential[1] per unit thickness of the respective monolayers. The monolayer thickness (dx) has been calculated from the difference in the numbers occurring at the vertical lines in the charge density plots in (a) and (b). The vertical lines have been positioned at the edges of the monolayers where the plane average charge denisty drops to zero. In other words, $\bar{\bar{V}}$ is the macroscopic electrostatic potential averaged over the volume of the individual monolayers.

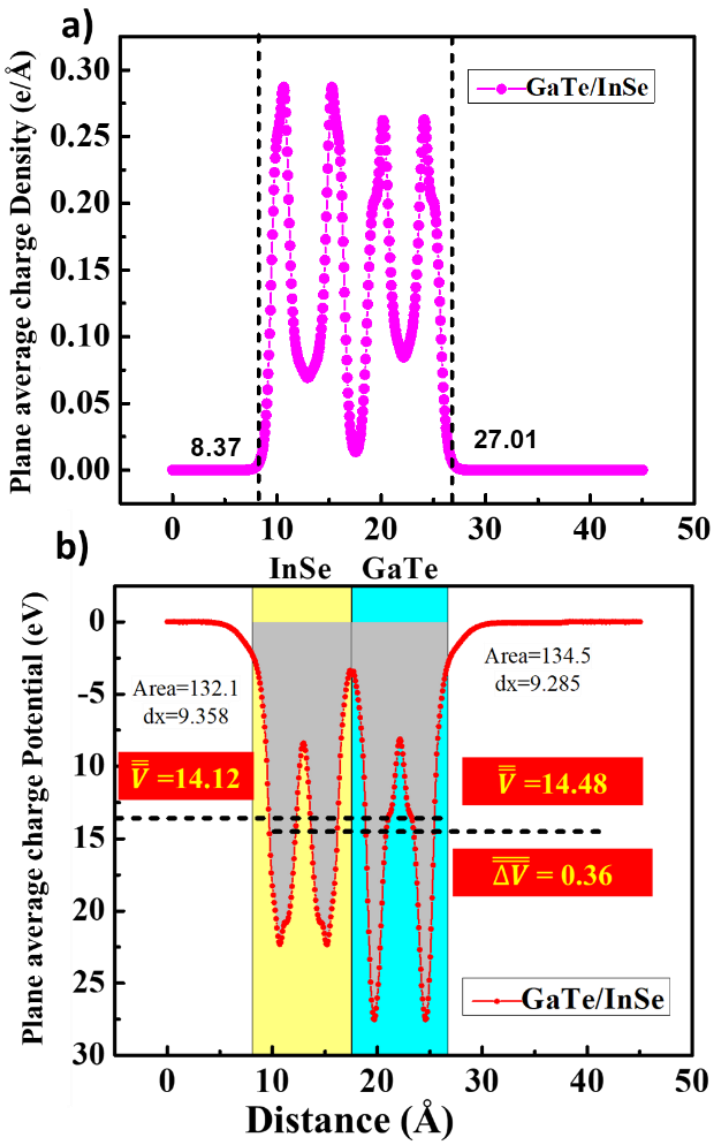

Figure S15. a) Plane average charge density and b) Potential of the heterostructure

The value of PCE is now calculated using the values metioned in Table S3.

$\Delta E_{CBO} = \overline{\overline{\Delta V}} + (E_{CBM} - \overline{\overline{V}})_{InSe} - (E_{CBM} - \overline{\overline{V}})_{GaTe}$

$\Delta E_{CBO} =$ 0.5 eV

Donor $E_g =$ 2.37 eV

PCE = 7.9%

The value of PCE using the isolated monoalyers is 9.1. Hence, both the approaches give nearly the same PCE values, which differ by 1-2%.

Reference

1. Liu, J.; Cheng, B.; Yu, J. A New Understanding of the Photocatalytic Mechanism of the Direct Z-Scheme g-C_3N_4/TiO_2 Heterostructure. *Phys. Chem. Chem. Phys.* **2016**, *18*, 31175–31183.